Supporting Information

Infiltration-assisted colloidal assembly of amorphous photonic crystal patterns with high color saturation and mechanical stability

Mengwei Xu[a], Ting Lü[a,b*], Dongming Qi[c], Ling Bai[d*], Ying Pan[a], Dong Zhang[a], Hongting Zhao[a]

[a]*Institute of Environmental Materials and Applications, College of Materials and Environmental Engineering, Hangzhou Dianzi University, Hangzhou 310018, China;*

[b]*Key Laboratory of Novel Materials for Sensor of Zhejiang Province, College of Materials and Environmental Engineering, Hangzhou Dianzi University, Hangzhou 310018, China;*

[c]*Key Laboratory of Green Cleaning Technology & Detergent of Zhejiang Province, Lishui 323000, Zhejiang, China;*

[d]*School of Material Science and Engineering, Jiangsu University, 301 Xuefu Street, Zhenjiang 212013, China.*

*Corresponding author: E-mail: lvting@hdu.edu.cn (Ting Lü) and lingmubai@ujs.edu.cn (Ling Bai)

Materials

Sodium hydroxide (NaOH), potassium peroxodisulfate (KPS), sublimed sulfur (≥99.5%), ethanol, sodium dodecyl sulfate (SDS), styrene (St), 3-(triethoxysilyl)propyl methacrylate (TESPMA, >98.0%), styrene (St), methyl methacrylate (MMA), acrylic acid (AA), methacrylic acid (MAA), butyl acrylate (BA) and tetrahydrofuran (THF) were purchased from Aladdin Chemistry Co., Ltd. 1,2,3-trichloropropane (TCP, ≥98%) and were purchased from Macklin Chemistry Co., Ltd. Pluronic F127 was purchased from BASF. All reagents were of analytical grade and used without further purification. Deionized water was used in all experiments.

Characterization methods

Transmission electron microscopy (TEM, JEM-2100F) or field emission scanning electron microscope (FESEM, FEI, Apreo S HiVac) was used to observe the morphology and size of the monodisperse PSF or PS particles and CLPA nanoparticles. The microscope with an SDD energy-dispersive spectroscopy (EDS) system was applied to map the TEM EDS element. FESEM was used to examine the microstructure of APC patterns, and its order degree of colloidal array was assessed in terms of the 2D Fast Fourier transform (2D-FFT) patterns. Fourier transform infrared (FTIR) spectrometer (Nicolet 6700, Thermo Fisher Scientific, USA) was used to determine the molecular structures of PSF and CLPA with potassium bromide pellet technique. Differential scanning calorimeter (DSC, TA Instruments, Model DSC Q2000) was used to measure the glass transition temperature (T_g) of PSF particles and CLPA nanoparticles. To eliminate its thermal history, the sample was heated to 150 °C at a rate of 20

°C/min and then stayed at 150 °C for 3 min. Thereafter, the temperature fell to −25 °C and then rised to 150 °C again at a rate of 20 °C/min. The curve of second heating run was used to determine the T_g. Reflection spectrometer (Ocean Optics HR2000+, or ideaoptics PG2000^{PRO}) was used to record the reflection spectra of APCs. Friction experiment was conducted to assess the mechanical stability of APC patterns. Briefly, the prepared APC patterns were rubbed five times by sandpaper (3000 meshes) which was loaded with a weight (100 g). Subsequently, their integrity and visual structural color of APC patterns were then observed carefully. Moreover, the mechanical stability was also characterized by buckling or ultrasonic washing for 30 min (ultrasonic power: 200 W).

Characterization of CLPA nanoparticles

The FTIR spectrum, DSC curve, TEM image and dissolvability evaluation of CLPA nanoparticles were shown in Figure S6. The size of CLPA nanoparticles was about 33 nm (Figure S6c). The C-H stretching vibrations of methylene groups was found at around 2937 and 2862 cm^{-1}, while its bending vibration was found at 1456 and 1387 cm^{-1}; the strong C=O vibration was observed at 1735 cm^{-1}, and the C–O–C symmetric and antisymmetric stretching vibration of was observed around 1245 and 1142 cm^{-1} (Figure S6a), respectively. Since only a very small amount of TESPMA was introduced, the Si–O–Si peak was not obvious. However, the cross-linked structure of dried CLPA nanoparticles could be confirmed by its solubility in THF solvent. Just as shown in Figure S6d, the PA nanoparticles without containing TESPMA could be completely dissolved in THF solvent, while the CLPA nanoparticles could not be dissolved in THF, which could be ascribed to the cross-linked

structure in CLPA nanoparticles induced by the hydrolysis and condensation of TESPMA. According to its DSC curve (Figure S6b), the T_g of CLPA nanoparticles was determiend to be around 16.4 °C. As a result, during its co-assembly process, the soft CLPA nanoparticles formed cross-linked films in the PSF particle gaps at room temperature, thereby promoting the mechanical stability of colloidal array.

Calculation of RI of PSF particles

In this study, the refractive index of PSF particles was calculated by Bragg's equation,[1] based on the reflection spectrum of an ordered photonic crystals (PCs) composed of PSF nanospheres. Herein, dip coating method was used to prepare PCs. Briefly, a clean glass slide was placed in an aqueous dispersion of 2 wt% colloidal particles and withdrawn by a motor at the speed of 1.0 mm/h for dip coating. The Bragg's equation was presented as follow:

$$n = \sqrt{\left[\left(\frac{\lambda_{max}}{\sqrt{8/3}\times D}\right)^2 - 0.26\right] \div 0.74}$$

where λ_{max} stands for the maximum reflection wavelength of colloidal photonic crystal, n stands for the refractive index (RI) of PSF particles, while D stands for the PSF particle size. According to Figure S8a and Figure S8b, the PCs composed of 245nm PSF spheres, showed a reflection peak of 656.1 nm, therefore the refractive index of PSF spheres was calculated to be 1.81, which is close to the data of previous works.[2]

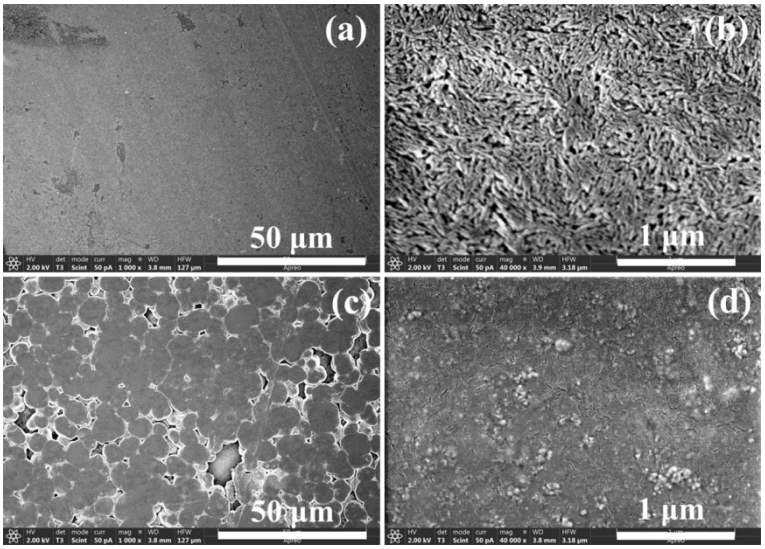

Figure S1 FESEM images of photo papers before (a, b) and after (c, d) hydrophobic treatment.

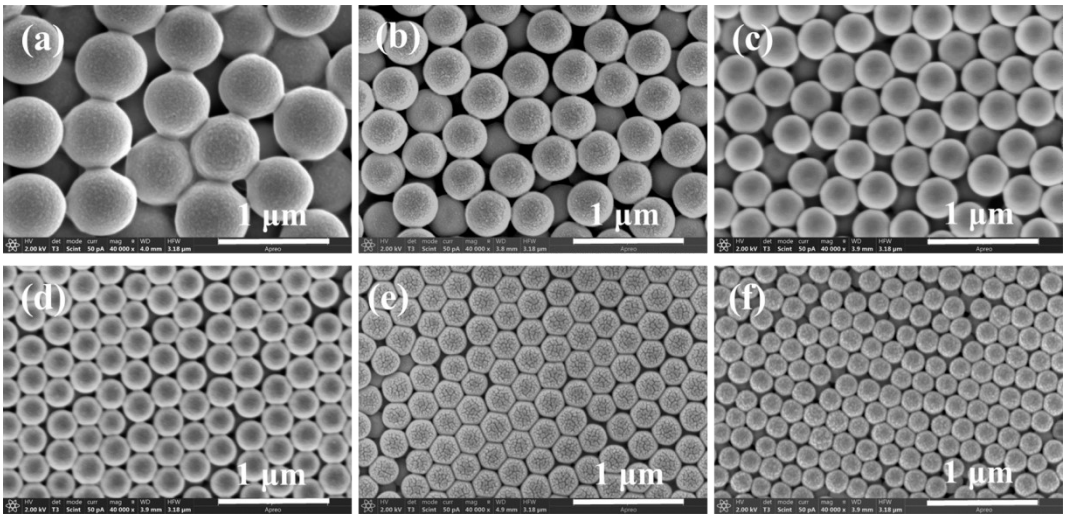

Figure S2 FESEM images of PSF nanospheres prepared at various temperatures: (a) 50 °C, (b) 60 °C, (c) 70 °C, (d) 75 °C, (e) 80 °C, (f) 85 °C.

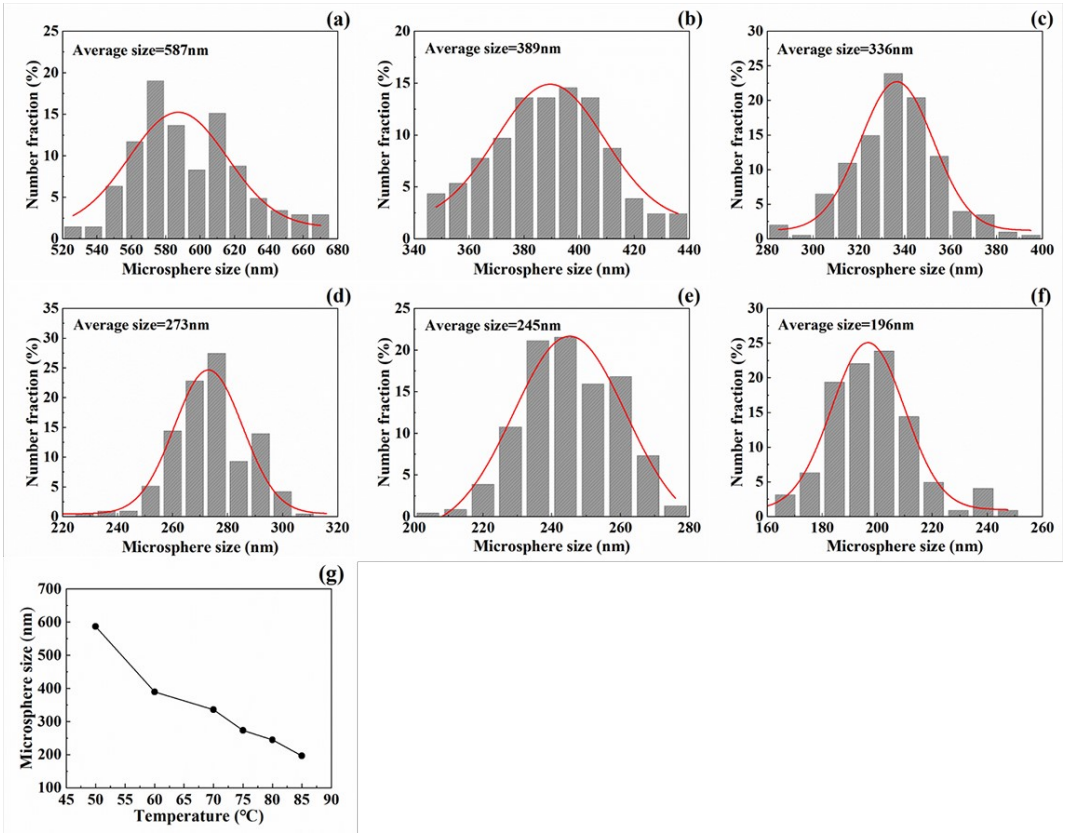

Figure S3 Size distribution of PSF nanospheres prepared at various temperatures: (a) 50 °C, (b) 60 °C, (c) 70 °C, (d) 75 °C, (e) 80 °C, (f) 85 °C, and effect of reaction temperature on the particle size (g)

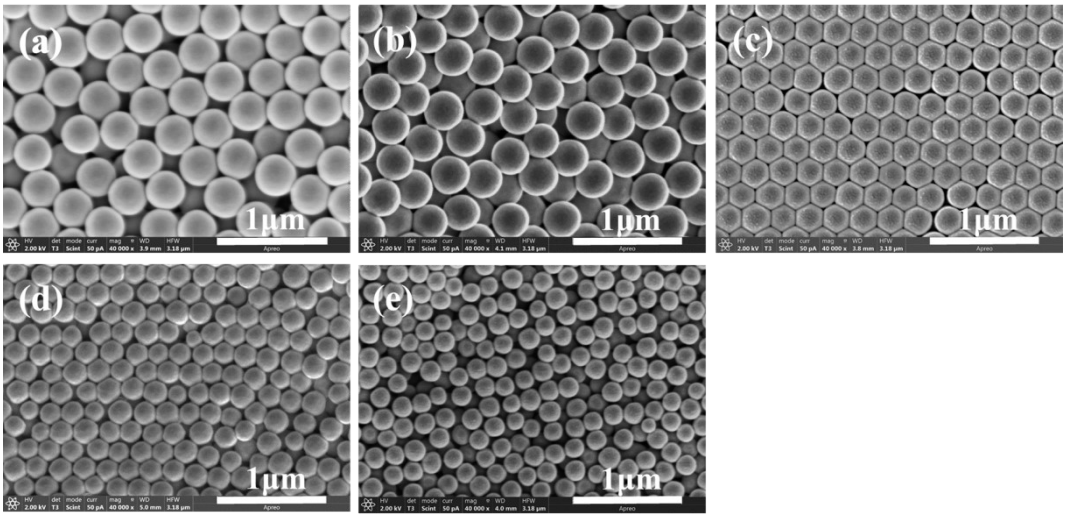

Figure S4 FESEM images of PSF nanospheres prepared at various ethanol/water ratios: (a) 90/160, (b) 80/170, (c) 70/180, (d) 60/190, (e) 50/200.

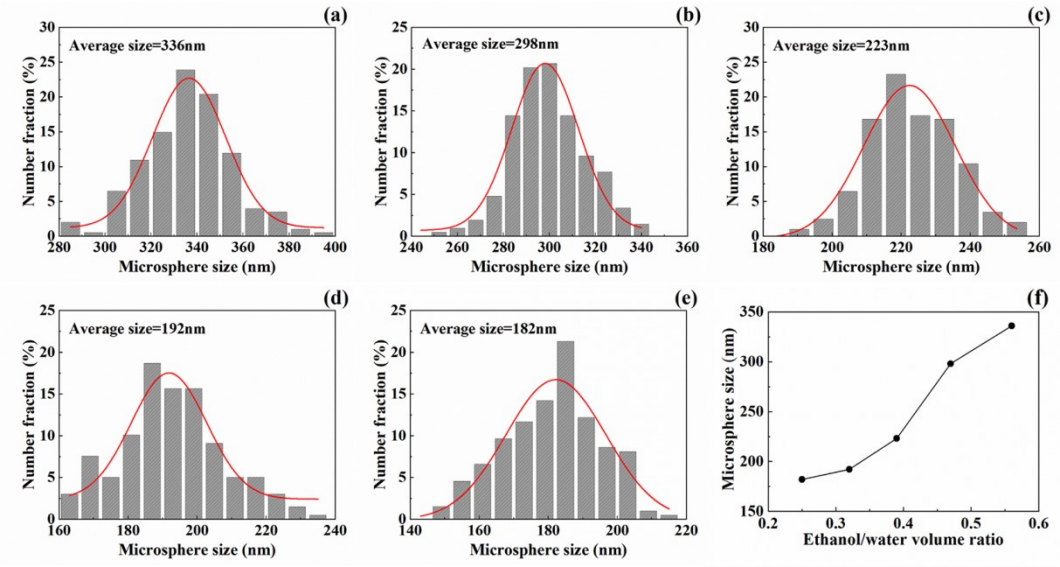

Figure S5 Size distribution of PSF nanospheres prepared at various ethanol/water ratios: (a) 90/160, (b) 80/170, (c) 70/180, (d) 60/190, (e) 50/200, and effect of ethanol/water ratio on the particle size (f)

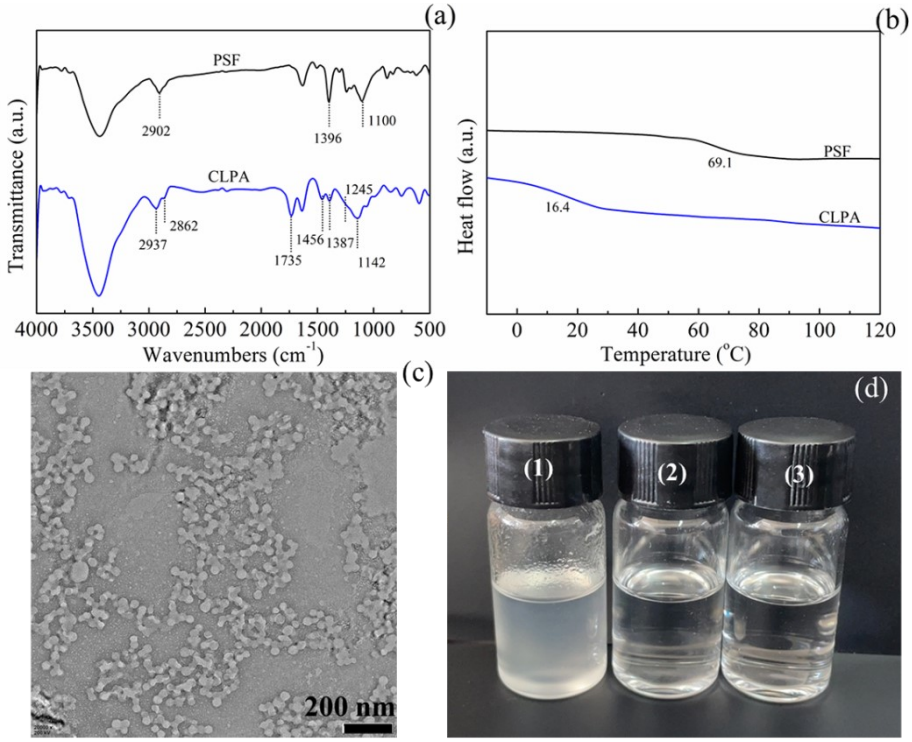

Figure S6 FTIR spectra (a) and DSC curves (b) of PSF nanospheres and CLPA nanoparticles, TEM image of CLPA nanoparticles (c), and dissolvability of nanoparticles in THF (d): CLPA nanoparticles in THF (1), PA nanoparticles in THF (2), THF solvent (3)

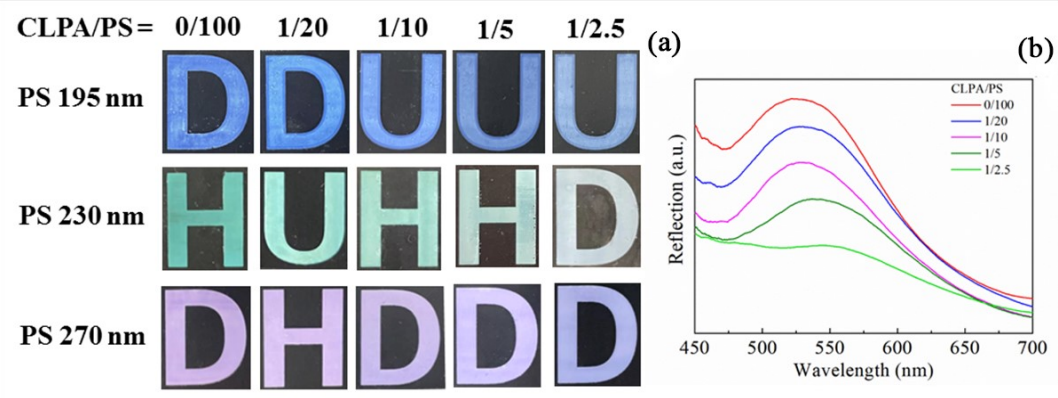

Figure S7 Photographs of APC letter patterns composed of different sized PS nanospheres and various contents of CLPA nanoparticles, and the reflection spectra of APCs prepared at different CLPA/PS (230 nm) ratios (b).

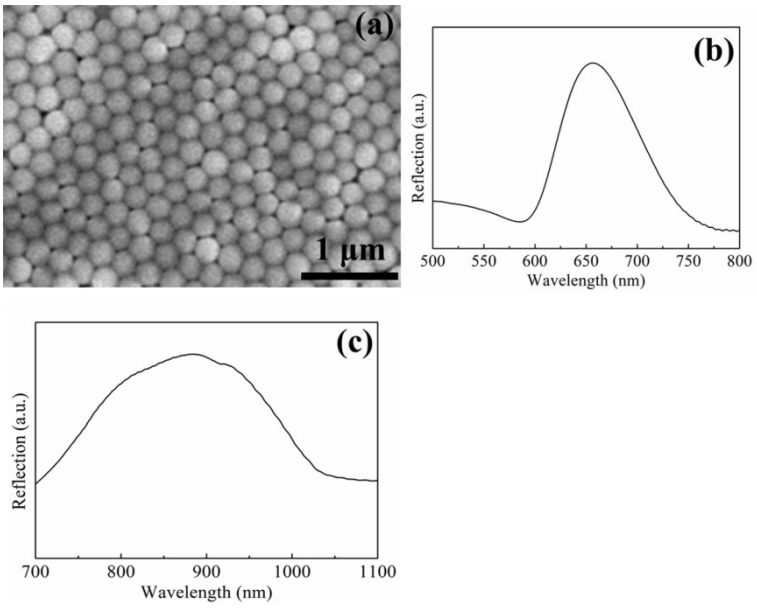

Figure S8. FESEM image of the ordered photonic crystal composed of PSF nanospheres (245 nm) (a) and corresponding reflection spectrum (b); near infrared region of the reflection spectrum of APCs composed of PSF nanospheres (273 nm).

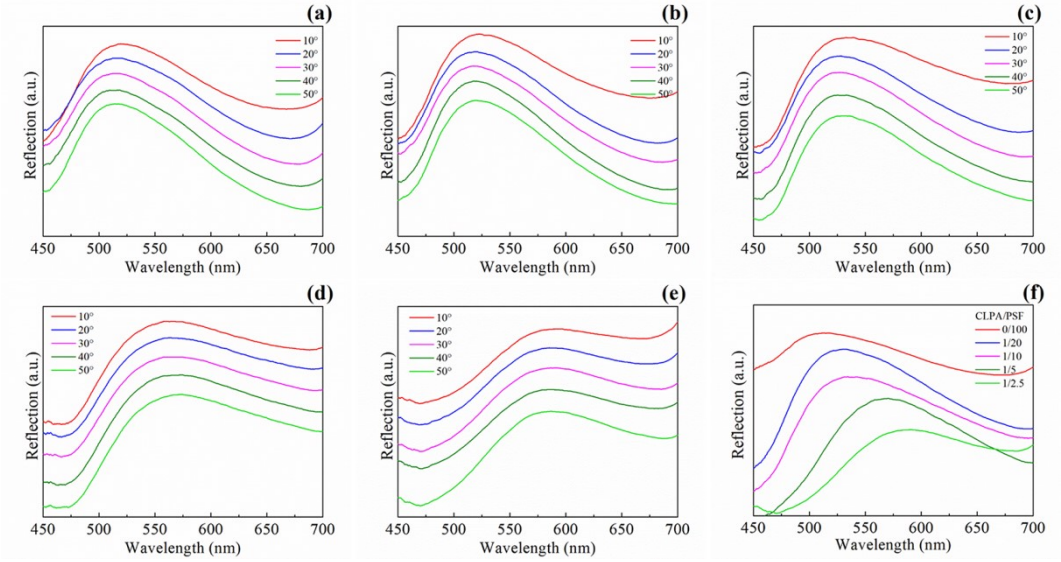

Figure S9. Reflection spectra of APCs composed of PSF nanospheres (196 nm) and CLPA nanoparticles at various CLPA/PSF ratios: (a) 0/100, (b) 1/20, (c) 1/10, (d) 1/5, (e) 1/2.5; reflection spectra of APC patterns after friction at different CLPA/PSF ratios (f).

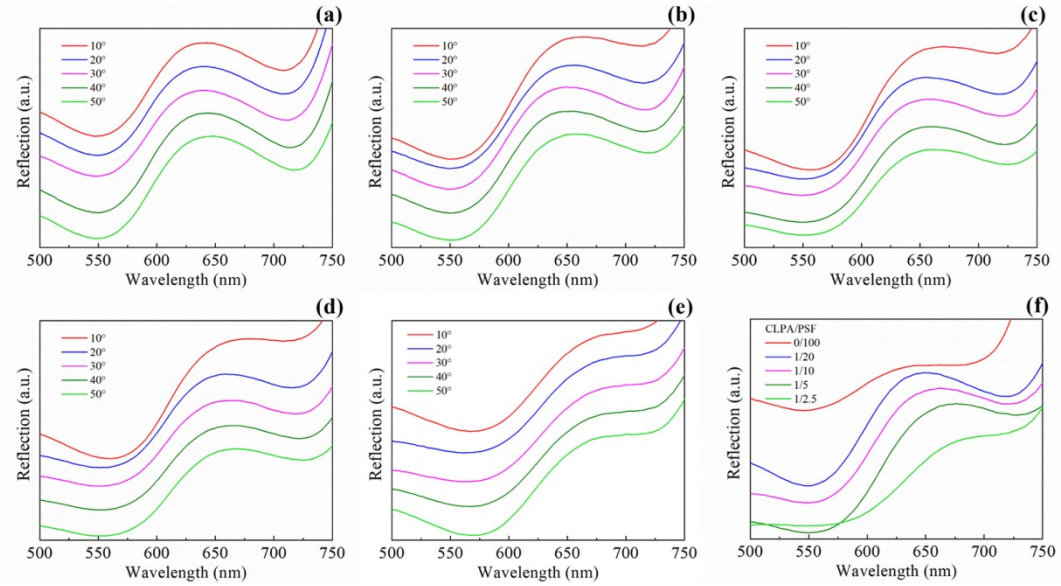

Figure S10. Reflection spectra of APCs composed of PSF nanospheres (245 nm) and CLPA nanoparticles at various CLPA/PSF ratios: (a) 0/100, (b) 1/20, (c) 1/10, (d) 1/5, (e) 1/2.5; reflection spectra of APC patterns after friction at different CLPA/PSF ratios (f).

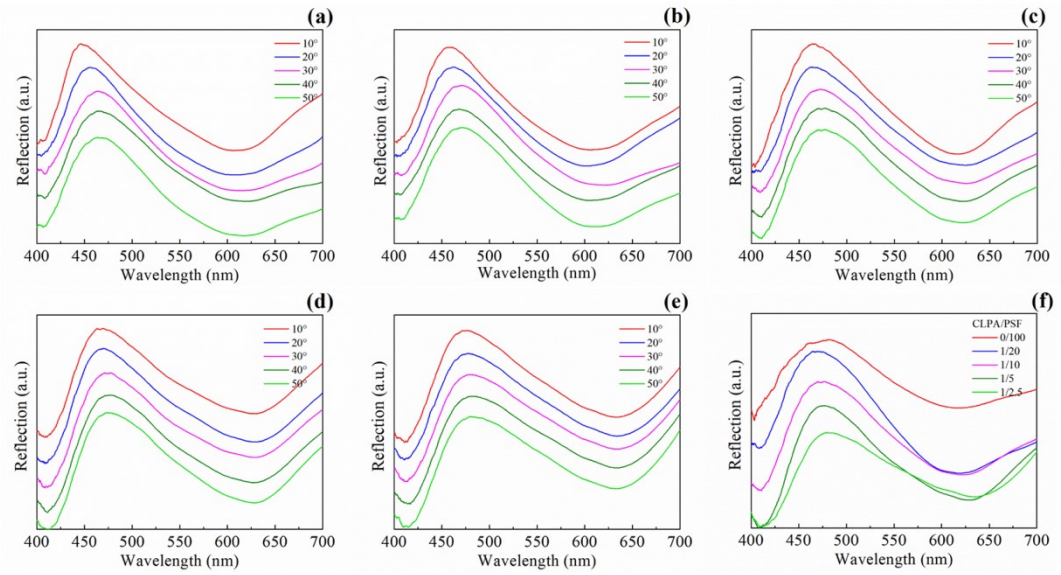

Figure S11. Reflection spectra of APCs composed of PSF nanospheres (273 nm) and CLPA nanoparticles at various CLPA/PSF ratios: (a) 0/100, (b) 1/20, (c) 1/10, (d) 1/5, (e) 1/2.5; reflection spectra of APC patterns after friction at different CLPA/PSF ratios (f).

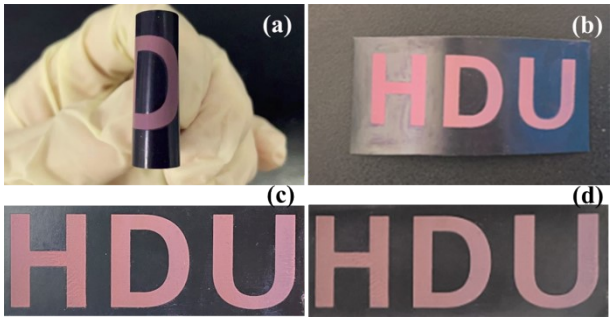

Figure S12. Photographs of APC letter patterns: (a) buckled pattern, (b) recuperative patterns after buckling; (c) original pattern before washing, (d) after ultrasonic washing

References

1 K. C. Lee, *J. Nanosci. Nanotechnol.*, 2019, **19**, 6334-6340.

2 F. Li, B. Tang, S. Wu and S. Zhang, *Small*, 2017, **13**, 1602565.